International Journal of Engineering, Mathematical and Physical Sciences
ISSN: 2517-9934
Vol:6, No:9, 2012

Free Convective Heat Transfer in an Enclosure Filled with Porous Media with and without Insulated Moving Wall

Laith Jaafer Habeeb

***Abstract*—**The present work is concerned with the free convective two dimensional flow and heat transfer, in isotropic fluid filled porous rectangular enclosure with differentially heated walls for steady state incompressible flow have been investigated for non-Darcy flow model. Effects of Darcy number ($0.0001 \leq Da \leq 10$), Rayleigh number ($10 \leq Ra \leq 5000$), and aspect ratio ($0.25 \leq AR \leq 4$), for a range of porosity ($0.4 \leq \varepsilon \leq 0.9$) with and without moving lower wall have been studied. The cavity was insulated at the lower and upper surfaces. The right and left heated surfaces allows convective transport through the porous medium, generating a thermal stratification and flow circulations. It was found that the Darcy number, Rayleigh number, aspect ratio, and porosity considerably influenced characteristics of flow and heat transfer mechanisms. The results obtained are discussed in terms of the Nusselt number, vectors, contours, and isotherms.

***Keywords*—**Numerical study, moving-wall cavity flow, saturated porous medium, different Darcy and Rayleigh numbers.

I. Introduction

A basic understanding of fluid flow and heat transfer in a lid-driven cavity filled with saturated porous medium with buoyancy effect for steady state case is important in many areas such as solar power collector, nuclear energy systems, chemical processing equipment, coating and industrial processes, galvanizing and metal coating, float glass manufacturing, dynamics of lakes and large reservoirs, crystal growth, food processing and so on. Numerous investigations have been conducted in the past on lid-driven cavity flow and heat transfer considering various combinations of the imposed temperature gradients and cavity configurations. Such configurations can be idealized by the simple rectangular geometry with regular boundary conditions yielding a well-posed problem. The resulting flow however, is rather complex even when the flow is purely shear driven for the isothermal case without any temperature gradient. When a temperature gradient is imposed such that the shear driven and buoyancy effects are of comparable magnitude then the resulting flow falls under the convection regime and the interaction and coupling of these effects makes the analysis more complex. In general, the current numerical models to predict the flow through porous media fall in four categories: the Darcy model, the Forcheimer model, the Brinkman model and the Brinkman-Forcheimer model.

Laith J. Habeeb is with the Mechanical Engineering Dept.,University of Technology, Baghdad – Iraq(e-mail: laithjaafer@yahoo.com , or, dr.laith_jaafer@uotechnology.edu.iq).

The Darcy model was developed based on the original Darcy equation. However, this model is reported to produce unsatisfactory results when compared with the theoretical prediction based on Darcy law. In forcheimer model, it considers the non-linear drag effect due to the solid matrix while the Brinkman model includes the viscous stress introduced by the solid boundary. Even though these two models have been widely used by many researchers, they are not general enough to be applicable for a medium with variable porosity. In recent years, the Lattice Boltzmann Method (LBM) has received considerable attention as an alternative approach for simulating wide range of fluid flow. Unlike other numerical methods, LBM predicts the evolution of particle distribution function and calculates the macroscopic variables by taking moment to the distribution function. Nithiarasu *et al* [1] outlined a double-diffusive natural convection in a fluid saturated porous medium using the finite element method. A generalized porous medium model was used to study both Darcy and non-Darcy flow regimes in an axisymmetric cavity. Results indicated that the Darcy number should be a separate parameter to understand flow characteristics in non-Darcy regime. The influence of porosity on heat and mass transfer was significant and the transport rates may differ by 25% or more, at higher Darcy and Rayleigh numbers. When compared with the Darcy and other specialized models of Brinkman and Forchheimer, the present generalized model predicted the least heat and mass transfer rates. It was also observed that an increase in radius ratio leads to higher Nusselt and Sherwood numbers along the inner wall. Hakan [2] performed a numerical work to analyze combined convection heat transfer and fluid flow in a partially heated porous lid-driven enclosure. The top wall of enclosure moves from left to right with constant velocity and temperature. Heater with finite length was located on the fixed wall where its center of location changes along the walls. The finite volume-based finite-difference method was applied for numerical experiments. Parameters effective on flow and thermal fields were Richardson number, Darcy number, center of heater and heater length. The results were shown that the best heat transfer was formed when the heater was located on the left vertical wall. Hakan [3] investigated numerically the natural convection heat transfer in a partially cooled and inclined rectangular enclosure filled with saturated porous medium. One of side wall has constant hot temperature and one adjacent wall is partially cooled while the remaining ones were adiabatic.

Finite volume based finite difference method was applied using the SIMPLE algorithm. Governing parameters were: Darcy Rayleigh number ($10 \le Ra \le 1000$), center of location of heater ($0.1 \le c \le 0.9$), inclination angle ($0^o \le \varphi \le 90^o$) and length of cooler ($0.25 \le w \le 0.75$). It was found that inclination angle was the dominant parameter on heat transfer and fluid flow as well as aspect ratio. Ayad [4] studied numerically two–dimensional, steady natural convection in a rectangular cavity filled with a heat generating saturated porous medium for the case when the vertical walls of the cavity were isothermal and the horizontal walls were either adiabatic or cold. Finite difference method was used to transform the momentum and energy equations from the differential form to the algebraic form; relaxation method was used to solve the momentum equation, while (L.S.O.R.) method was used to solve the energy equation for Rayleigh No. ranges ($10 \le Ra \le 10^4$). Results were presented in terms of the stream lines and isotherms, the maximum temperature in the cavity and intermediate Nusselt number. The thermal convection flow together with the uniform heat generating produces a highly stratified medium at high Rayleigh numbers. The change in the horizontal wall boundary condition from adiabatic to cold reduces (θ_{max}) also it was found that heat transfer increase with increasing Rayleigh number while it decrease with aspect ratio. The effect of aspect ratio on heal transfer will appear when ($Ra > 50$). Wang [5] studied the lid-driven rectangular cavity containing a porous Darcy–Brinkman medium.

The governing equation was solved by an eigen function method which is much simpler than using biorthogonal series. It was found that the porous medium effect decreases both the strength and the number of recirculating eddies, especially for deep cavities. Mohd *et al* [6] investigated fluid flow behavior through porous media in a lid-driven square cavity. The Brinkman-Forcheimer equation was coupled with the lattice Boltzmann formulation to predict the velocity field in the system. Three numerical experiments were performed with different values of Darcy number to investigate the effect of porosity on the fluid flow. They found that the magnitude of velocity, strength of vortex and velocity boundary layer was significantly affected porosity of the media. The lattice Boltzmann simulation scheme was capable in prediction of fluid flow behavior through porous media. Mohamed and Wael [7] concerned with the mixed convection in a rectangular lid-driven cavity under the combined buoyancy effects of thermal and mass diffusion.

Double-diffusive convective flow in a rectangular enclosure with moving upper surface is studied numerically. Both upper and lower surfaces are being insulated and impermeable. Constant different temperatures and concentration are imposed along the vertical walls of the enclosure. The numerical results are reported for the effect of Richardson number, Lewis number, and buoyancy ratio on the iso-contours of stream line, temperature, and concentration. In addition, the predicted results for both local and average Nusselt and Sherwood numbers are presented and discussed for various parametric conditions.

MOHD [8] applied (LBM) to predict the phenomenon of natural convection in a generalized isotropic porous media model filled in a square geometry by introducing a force term to the evolution equation and porosity to the density equilibrium distribution function. The temperature field was obtained by simulating a simplified thermal model which useslessvelocity directions for the equilibrium distribution function and neglects the compression work done by the pressure and the viscous heat dissipation. The model was used for simulation at ε equal to 0.4, 0.6 and 0.9. The results obtained were discussed in terms of the Nusselt number, streamlines and isotherms. Comparison with previous works confirms the applicability of the model. Waheed *et al* [9] investigated numerically the mixed convective heat transfer in a fluid-saturated porous medium using the generalized non-Darcy model. The flow governing parameters including the Darcy, Richardson and Péclet numbers, and the length-to-height aspect ratio were varied in the range $10^{-3} \le Da \le 10$, $0.1 \le Ri \le 10$, $1 \le Pe \le 10^3$ and $0.5 \le AR \le 4$ respectively while the Reynolds number was held constant at a value of $Re = 100$ for all computations. The results showed that all the flow governing parameters have strong influence on the flow pattern and heat distribution within the enclosure. Prakash and Satyamurty [10] investigated the free convective flow and heat transfer, in an anisotropic fluid filled porous rectangular enclosure using Brinkman extended non-Darcy flow model. The studies involve simultaneous consideration of hydrodynamic and thermal anisotropy. Numerical solutions employing the successive accelerated replacement (SAR) scheme have been obtained for $100 \le Ra \le 1000$, $0.5 \le AR \le 5$, $0.5 \le K^* \le 5$, $0.5 \le k^* \le 5$, and $0 \le Da \le 0.1$. It has been found that average Nusselt number increases with increase in K^* and decreases as $k*$ increases. However, the magnitude of the change in average Nusselt number depends on the parameter *Da*, characterizing the Brinkman extended non-Darcy flow. Antonio [11] used lattice-Boltzmann equation method to simulate non-Darcy flow in porous media. 2-D in-line and staggered arrangements of uniform cylinders have been considered. The results of a comprehensive computational evaluation were reported: the range of validity of Darcy-Forchheimer equation was investigated and correlations for macroscopic transport properties were presented (i.e., for the permeability and the inertial parameter). His investigation covered both no-slip and the slip-flow regimes. Wenchao and Yueying [12] built dimensionless mathematical models of one-dimensional flow in the semi-infinite long porous media with threshold pressure gradient for the two cases of constant flow rate and constant production pressure on the inner boundaries. Through formula deduction, it was found that the velocity of the moving boundary is proportional to the second derivative of the unknown pressure function with respect to the distance parameter on the moving boundary, which is very different from the classical heat-conduction Stefan problems. However, by introducing some similarity transformation from Stefan problems, the exact analytical solutions of the dimensionless mathematical models were obtained, which can be used for strict validation of approximate analytical solutions, numerical solutions and pore-scale network modeling for the flow in porous media with threshold pressure gradient.

Comparison curves of the dimensionless pressure distributions and the transient dimensionless production pressure under different values of dimensionless threshold pressure gradient were plotted from the exact analytical solutions of problems of the flow in semi-infinite long porous media with and without threshold pressure gradient. It was shown that for the case of constant flow rate the effect of the dimensionless threshold pressure gradient on the dimensionless pressure distributions and the transient dimensionless production pressure was not very obvious; in contrast, for the case of constant production pressure the effect on the dimensionless pressure distributions was more obvious especially at the larger dimensionless distance near the moving boundary; and for the case of constant production pressure, the smaller the dimensionless threshold pressure gradient was, the larger the dimensionless pressure is, and the further the pressure disturbance area reached.

From the available literature, it is clear that the study of moving lower wall of an enclosure filled with porous medium with wide range of Darcy and Rayleigh numbers are limited. So, my concern in this work is to study the effects of Darcy number,Rayleigh number, and aspect ratio for a range of porosity with and without moving lower wall.

II. Problem Definition and Governing Equations

A. Physical model

A schematic of the system in the present study is shown in Fig. (1). The system consists of a square enclosure with sides of length H, filled with a fluidsaturated porous mediumand Prandlt number (*Pr*) =1.0. The problem has been studied assuming that the gravitational acceleration acts in the negative *y*-direction. As the square enclosure are long enough, so the flow is consider to betwo dimensional,the fluid and the solid matrix are in thermal equilibrium, and the porous medium is homogeneous.This study will be limited to: steady state incompressible fluid flow, square enclosure with differentially heated walls, isotropic porous media, and non-Darcy region.

The directions of vortex rotation generated under the 84 different conditions were examined.Always the left and right walls are subjected to hot and cold temperatures respectively, and the upper and lowerwalls are insulated (assumed to be adiabatic). The moving lid or wall is considered to be the lower one,which is moved to the right (+*x* direction).

In cases (1-18) no wall movementis applied for Darcy number (*Da* = 0.0001, 0.001, 0.01, 0.1 1.0, and 10.0) each at porosity (ε = 0.4, 0.6, and 0.9) and Rayleigh number (*Ra* = 10^4).

In cases (19-36) the lower wall is moving at 0.2 m/s and for Darcy number (*Da* = 0.0001, 0.001, 0.01, 0.1 1.0, and 10.0) each at porosity (ε = 0.4, 0.6, and 0.9) and Rayleigh number (*Ra* = 10^4) to study the movement effect.

In cases (37-54) again no wall movement is considered for Rayleigh number (*Ra* = 10, 50, 100, 500, 1000, and 5000) each at porosity (ε = 0.4, 0.6, and 0.9) and Darcy number (*Da* = 0.01).

In cases (55-72) the lower wall is moving at 0.2 m/s and again for Rayleigh number (*Ra* = 10, 50, 100, 500, 1000, and 5000) each at porosity (ε = 0.4, 0.6, and 0.9) and Darcy number (*Da* = 0.01)to show the movement effect.

In cases (73-78),a stationary wall is required at (*Ra* = 1000), (*Da* = 0.01),and aspect ratio (*AR*= 0.25 and 4.0)each at porosity (ε = 0.4, 0.6, and 0.9) respectively.

In cases (79-84),a moving wall is required at (*Ra* = 1000), (*Da* = 0.01),and aspect ratio (*AR*= 0.25 and 4.0)each at porosity (ε = 0.4, 0.6, and 0.9) respectivelyto study the movement effect.

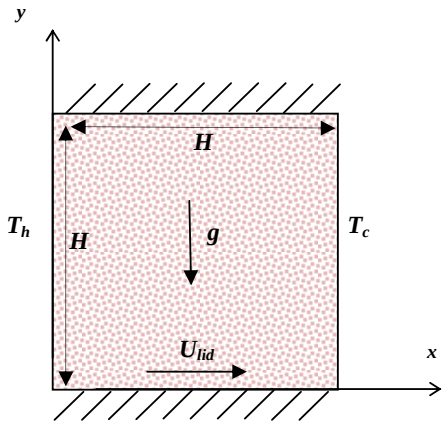

Fig. 1 Schematic diagram for the physical modelwith the wall boundary constraints and the coordinate axes

B. Materials and methods

Following [6], [8], and [13] the generalized model for incompressible fluid flow through porous media can be expressed by the following equations:

$$\nabla \cdot u = 0 \tag{1}$$

$$\partial u/\partial t + (u \cdot \nabla)(u/\varepsilon) = -(1/\rho)\nabla(\varepsilon\, p) + \upsilon_\varepsilon \nabla^2 u + F \tag{2}$$

F represents the total body force due to the presence of porous media and is given by:

$$F = -(\varepsilon\upsilon/K)u - \left(1.75/\sqrt{150\,\varepsilon K}\right)|u|\,u + \varepsilon\, G \tag{3}$$

The permeability (*K*) of which can be related to no dimensional parameter of Darcy number *Da* as follow:

$$K = Da \times H^2 \tag{4}$$

In the formulation of LBM, the starting point is the evolution equation, discrete in space and time, for a set of distribution functions *f*. If a two-dimensional nine-velocity model (D2Q9) is used for flow field and two-dimensional four-speed (D2Q4) Lattice Boltzmann equation(LBE)model is used to simulate the temperature field, then the evolution equations for a given *f*and *g* takes the following forms:

$$f_i(x+e_i\Delta t,t+\Delta t)-f_i(x,t)= -1/\tau_f\left[f_i(x,t)-f_i^{eq}(x,t)\right]+F_i \quad (5)$$

$$g_i(x+e_i\Delta t,t+\Delta t)-g_i(x,t)= -1/\tau_g\left[g_i(x,t)-g_i^{eq}(x,t)\right] \quad (6)$$

Where i = 0,1,…,8 for f and i = 1,2,3,4 for g.

Where distribution functionf_is used to calculate density and velocity fields while distribution function is used to g_i to calculate temperature field. Here, e denotes the discrete velocity set and expressed as:

$$e_i=\begin{cases}(0,0), & i=0\\ (\pm 1,0),(0,\pm 1), & i=1-4\\ (\pm 1,\pm 1), & i=5-8\end{cases} \quad (7)$$

f_i^{eq},$g_i^{eq}$are equilibrium distribution functions, the choice of which determines the physics inherent in the simulation. For D2Q9 and (D2Q4) models, $f_i^{eq}$and$g_i^{eq}$are expressed as:

$$f_i^{eq}=\rho\omega_i\left[1+3e_i\cdot u+(9/2)((e_i\cdot u)^2/\varepsilon)-(3/2)((u)^2/\varepsilon)\right] \quad (8)$$

$$g_{1,2,3,4}^{eq}=\rho T(1/4)\left[1+(e_i\cdot u/c^2)\right] \quad (9)$$

Where, the weights areω_0= 4/9,$\omega_{1\text{-}4}$= 1/9 and $\omega_{5\text{-}8}$= 1/36. The time relaxation and the effective viscosity can be related as follow:

$$\upsilon_\varepsilon=(1/3)(\tau-(1/2)) \quad (10)$$

In order to obtain the correct macroscopic governing equations, the forcing term $F_i$must be expressed in terms of medium porosity as follow:

$$F_i=\rho\omega_i(1-(1/2\tau))\cdot\left[3e_i\cdot F+(9(uF:e_ie_i)^2/\varepsilon)-(3u\cdot F/\varepsilon)\right] \quad (11)$$

The macroscopic density and the macroscopic flow velocity can then be calculated as follow:

$$\rho=\sum_{i=1}^{9} f_i^{eq} \quad (12)$$

$$v=\sum_i e_i f_i/\rho+(\varepsilon G/2) \quad (13)$$

and:

$$u=v/\left(c_0+\sqrt{c_0^2+c_1|v|}\right) \quad (14)$$

where:

$$c_0=(1+\varepsilon\upsilon/2K)/2 \quad and \quad c_1=1.75\varepsilon/2\sqrt{150\varepsilon^2K}$$

It is noted that, if we set ε= 1, the Lattice Boltzmann equation reduces to the standard equation of free fluid flows.

Boussinesq approximation is applied to the buoyancy force term. With this approximation, it is assumed that all fluid properties are constant except for density change with temperature.

$$G=\beta g(T-T_m)j \quad (15)$$

The dynamical similarity depends on three dimensionless parameters: the Prandtl number (*Pr*), Rayleigh number (Ra) and Nusselt number (*Nu*).

$$Pr=\upsilon/\chi \quad (16)$$

$$Ra=\rho\beta(T_h-T_c)L^3/\upsilon\chi \quad (17)$$

$$Nu=(H/\chi\Delta T)(1/H^2)\int_0^H\int_0^H q_x(x,y)dx\,dy \quad (18)$$

Where: $q_x(x,y)=uT-\chi(\partial/\partial x)T(x,y)$is the local heat flux in *x*-direction.

III. Numerical Simulation

The present algorithmused is the same in [8] and [13], itbegin with main program with seven subroutines. The program is modified to fulfill the required different present cases and to handlemore complex geometries. The numerical data obtained for each node are used to plot graphical representation of vectors, contours and isotherms.Simulations were done by programming which uses Fortran PowerStation 4.0 (Microsoft Developer Studio). Desktop PC with Intel (R) Core(TM)2 Quad CPU, 3GHz processor and 4.00 GB RAM was used to run the simulation.

Numerical stability and iteration to converge need the particles to be at equilibrium state. This will be obtained by manipulating the value of the time relaxation. The value of time relaxation needs to be closer to 1 (1.1).

The closer time relaxation to 1, the more number of particles will be exchanged to equilibrium state. The main iteration is repeated until a convergence solution is obtained at convergence criteria for the velocity less than 1×10^{-8}. In the simulations, mesh sizes (101×101), (201×51), and (51×201) were used for cases (1-72), (73-75 & 79-81), and (76-78 & 82-84) respectively.

The calculations of average Nusselt numbers for the present program are compared early by [8]or [13] with other single phase fluid resultsfor different values of Rayleigh numberand the present Lattice Boltzmann model for simulation of Brinkman-Forchheimer equation is verified. The comparison showed that the obtained Nusselt number is acceptable.

IV. Results and Discussion

The results are presented for (84) different cases corresponding to *thirty six*Darcy-porosity effects, moreover to *thirty six*Rayleigh-porosity relationshipsand *twelve*aspect ratio-porosity arrangementsall with and without moving wall.

The best case of moving wall is when the lower wall is moving to the right and the maximum heat transfer occurs at 0.2 m/s as concluded in [13] for *Ra* =1000, ε=0.7, and *Da* =0.01.Thus in this work at moving wall cases, the lower wall is moving to the right at 0.2 m/s. The basic features of flow and heat transfer are analyzed with the help of the vectors, contour patterns and isothermal contours.Also, average Nusselt numbers for all cases are tabulatedand velocity components are plotted.Some of the results (that I find paper to compare with) have the same behavior of the similar published cases. Heat transfer in low speed lid-driven cavity flow is treated mostly as mixed convection. The flow driven by the movement of the wall is creating a forced convection conditions while temperature difference across the cavity causes a buoyancy driven, secondary flow. Thus, complicated patterns of heat and mass transfer occur inside the cavity.

A. Darcy number and movement effect

Fig.(2)showsthe velocity vectorsand temperature contours for the stationary wall for the square cavity filled with porous medium at *Ra* =10^4 and thermal diffusivity (χ = 0.2) .Fig. (2-A and B) show the velocity vectors with *y*-component velocity contours and temperature contours respectively for *Da* = 0.0001 and ε = 0.4.The vectors form a clockwise unicellular circulating flow pattern. One big upper clockwise vortex is appeared because of the density effect due to heating.For the isotherms, it can be observed that they are mostly parallel to the vertical hot and cold walls indicating that conductive heat transfer dominates. Fig. (2-C) predicts the velocity vectors with *y*-component velocity contours for *Da* = 0.0001 and ε = 0.9.Porosity does not seem to significantly affect the pattern only for the vortex center to be moved upward.Fig. (2-D) illustrates the temperature contours for *Da* = 0.01 and ε = 0.6.As the Darcy number and the porosity increase, there is a tendency of the lines to becoming less parallel. This is due to the fact that the inertial and non-linear drag terms are becoming less significant as the porosity increases, leading to higher dimensionless flow velocities which start to initiate convection. Also, at a lower Darcy number of 10^4, the velocity vectors (not shown here) are seen to violate the no-slip condition, with maximum magnitude near the wall. This is a typical characteristic of approximately Darcian flow regime. With increase in Darcy number 10^2, the flow satisfies the no-slip boundary condition on the walls. The point to be noted here is , the present generalized flow model predicts both the slip flow at lower Darcy numbers (near Darcian regime) and the no-slip flow condition at higher Darcy numbers (non-Darcian flow regime).Fig. (2-E) shows the velocity vectors with *y*-component velocity contours for *Da* = 1.0 and ε = 0.4.The elliptic shape of the vectors or of the vortex flow and the circular shape of the *y*-component velocity contours are now obvious. As the Darcy number and porosity increase, the circular shape vortex becomes more elliptic.

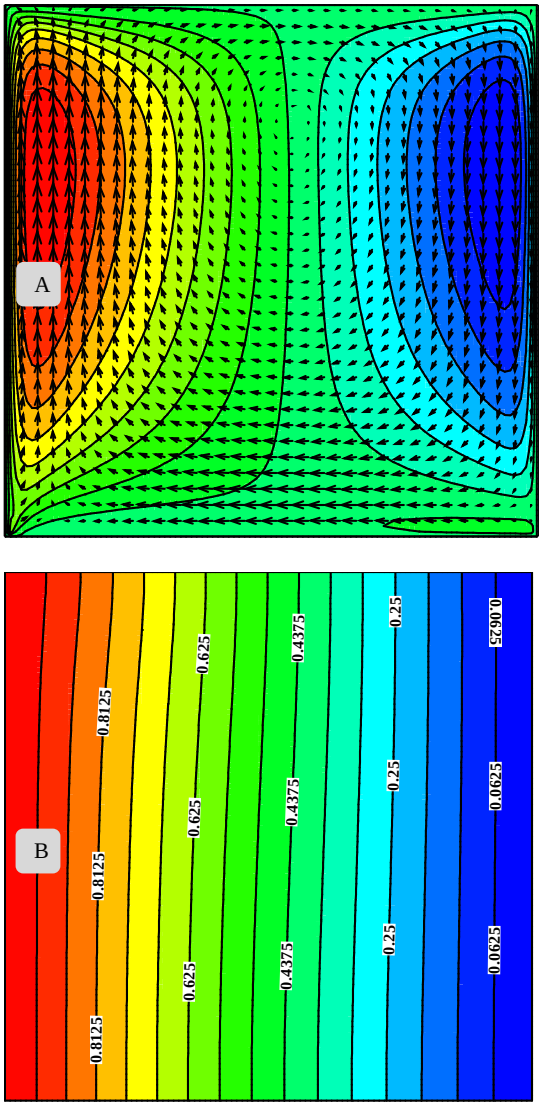

Fig. (3) shows the temperature contours and velocity vectors for the lower wall movement for the square cavity filled with porous medium at *Ra* = 10^4 and thermal diffusivity (χ = 0.2).

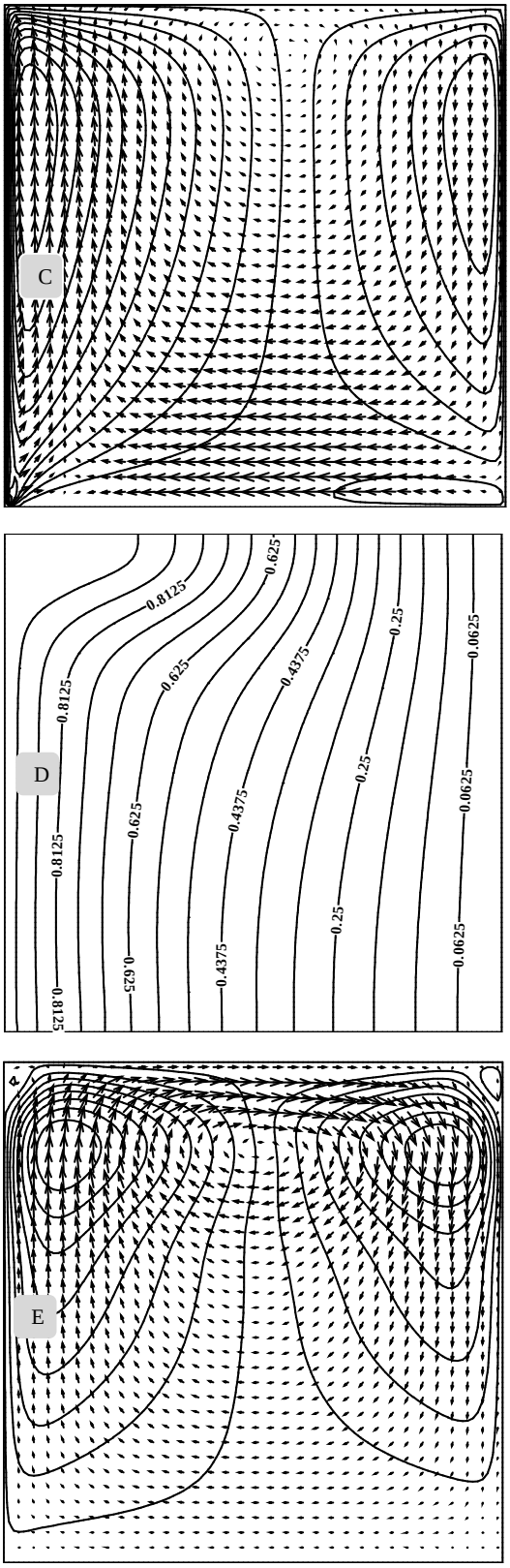

Fig. 2 Velocity vectors, contours and temperature contours for stationary wall cavity at $Ra = 10^4$

Fig. (3-A, B, and C) shows the temperature contoursat Da = 0.0001 and ε = 0.4, 0.6, and 0.9 respectively.It is obvious that the lines are now mostly curvature. Convection dominates at this Rayleigh number condition and as the porosity increase; the curvature effect becomes stronger due to the fact that the inertial and non-linear drag terms are becoming less significant as the porosity increases, leading to higher dimensionless flow velocities which make convection more vigorous. However at areas near to the walls, heat conduction still dominates. The viscous effect from the walls retards the momentum of buoyancy force initiated by the differentially heated walls which slows down convective effect. The moving lid transfers the heat from the left side and the vortex caries the heat to the center.Fig. (3-D) predicts the velocity vectorsat Da = 0.01 and ε = 0.9. When the lower wall moves to the right, two counterclockwise vortices are generated in the whole domain and a small clockwise vortex is generated near the left wall. Fig. (3-E) illustrates the temperature contoursat Da = 10.0 and ε = 0.9. As it shown, the isotherms aredistributed in whole domain resulting high Nusselt number.

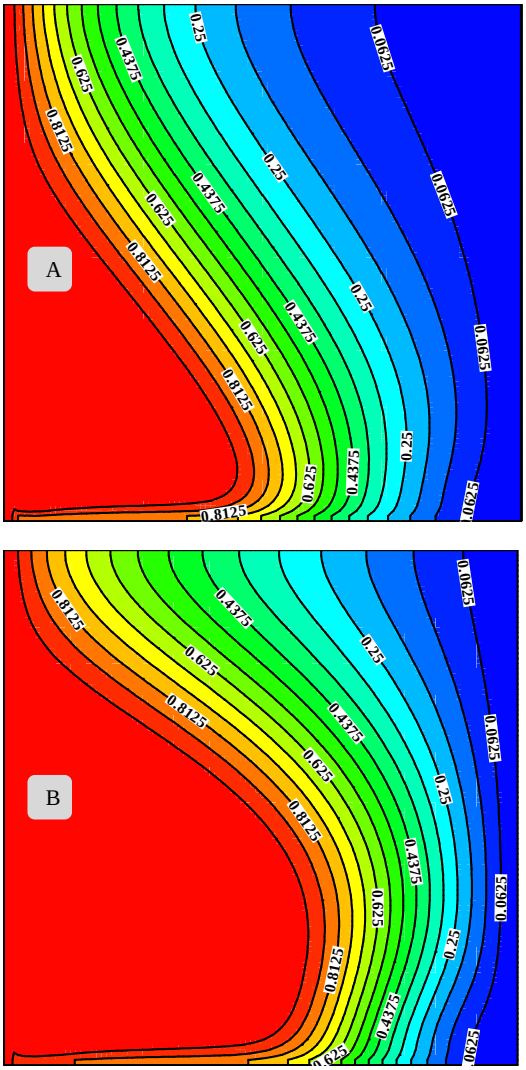

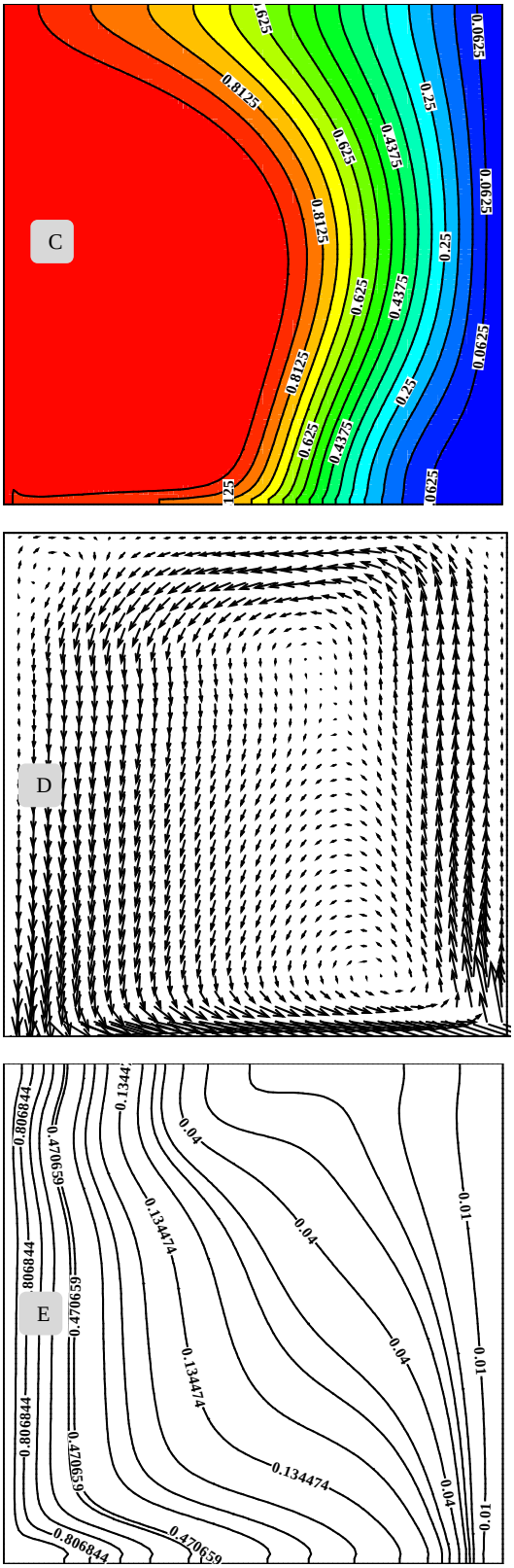

Fig. 3 Temperature contours andvelocity vectorsfor moving lower wall cavity at$Ra = 10^4$

Fig. 4 shows the relationship between the average Nusselt numberand Darcy numberwith and without movement at various porosities.When the Darcy number increases, the average Nusselt number is increases. But a significant increase in the average Nusselt number is detected at Darcy number range (0.0001-0.01) after that a small increase is noticed. As porosity increases, the average Nusselt number increases. A large increase in average Nusselt number is obtained when the lower wall is moved.

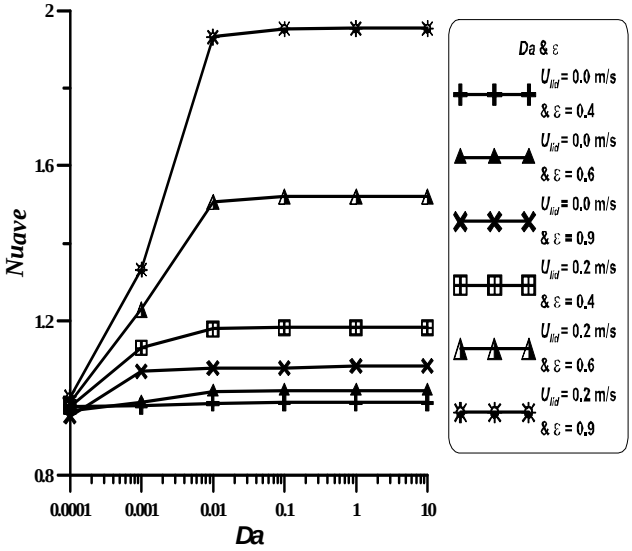

Fig. 4 Average Nusselt number and Darcy numberwith and without movement

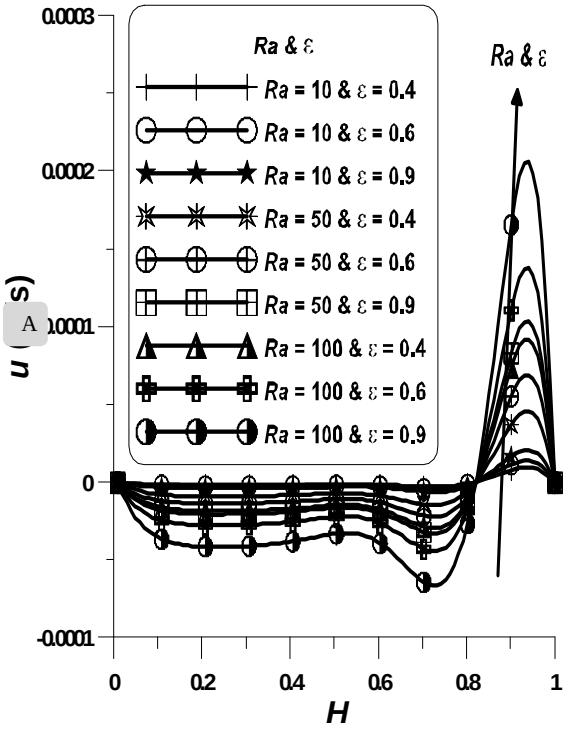

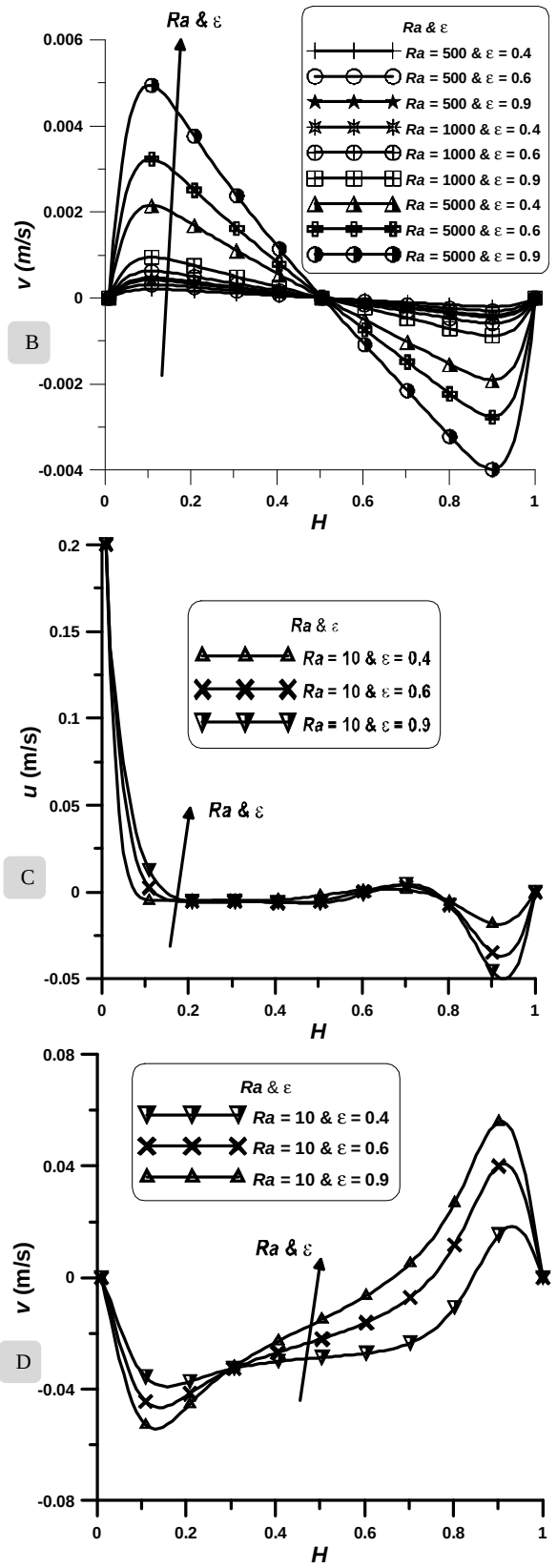

Fig. 5 Velocitiesdistributionsat different *Ra*and ε

B. Rayleigh number and movement effect

Fig. 5 shows the velocities distributions(*u*) or *x*-component along the box *height*and (*v*) or *y*-component along the box *width*for*Da* = 0.01 with and without movement.

Velocity components are plotted at mid width of the cavity and mid-height of the cavity respectively at different Rayleigh number and porosity.Fig. (5-A) shows the velocity distributions (*x*-component) for Ra = 10, 50, and 100and ε = 0.4, 0.6, and 0.9 without movement. At the top of the cavity, a significant increase in *x*-component velocity as Rayleigh number and porosity are increase.Fig. (5-B) shows the velocity distributions (*y*-component) for Ra = 500, 1000, and 5000 and the same porosity range without movement. A significant increase in *y*-component velocity as Rayleigh number and porosity are increase in the left hand side (+ values) and R.H.S. (- values).Fig. (5-C) shows the *x*-component velocity for Ra = 10and ε = 0.4, 0.6, and 0.9 with movement.

The velocity of the flow is higher near the hot vertical wall and it decreases continually with an increase in the horizontal distance.Fig. (5-D) shows the *y*-component velocity for Ra = 10 again at the same porosity range. The velocity of the flow is higher at the upper half of the cavity than that of bottom half.In the moving wall cases, a small increase in the velocity components due to *Ra*increase because of the high velocity magnitude of the moving wall comparing with the velocitiesof natural convection without movement.

C. Aspect ratio and movement effect

Fig. 6depicts the velocity vector with *y*-component velocity contours and temperature contour for *AR* = 0.25 and 4.0 at*Ra* = 1000 and *Da* = 0.01 with and without lower wall-driven. Fig. (6-A and B) show the velocity vectors with *y*-component velocity contours and temperature contours respectively at *AR* = 0.25 and ε = 0.4 without movement.

One big clockwise vortex is appeared in the middle of the cavity approximately.

The isotherms are being curvature near the hot wall and become vertical wherever it gets closer to the cold wall. Fig. (6-C) illustrates temperature contoursat *AR* = 0.25 and ε = 0.9again without movement. More curvature isotherms are being observedwith higher temperatures near the hot wall. Fig. (6-D, E, and F) shows velocity vectorswith*y*-component velocity contours at *AR* = 0.25 and ε = 0.4, 0.6, and 0.9 respectively withlower wall-driven.When porosity increases, movement would be spread well and vortex is formed to transfer fluid and heat.

Fig. (6-G and H) shows velocity vectors and*y*-component velocity contours at *AR* = 4.0 and ε = 0.6 without movement.For a deep cavities there exists a string of eddies of rapidly decreasing strength.Note that the strengths of the deep eddies are very small, thus has little effect on the transport properties of the cavity.Fig. (6-I and J)illustratesvelocity vectors and*y*-component velocity contours at *AR* = 4.0 and ε = 0.9 with lower wall-driven. More relevant is the dominant eddy adjacent to the moving lid.

A

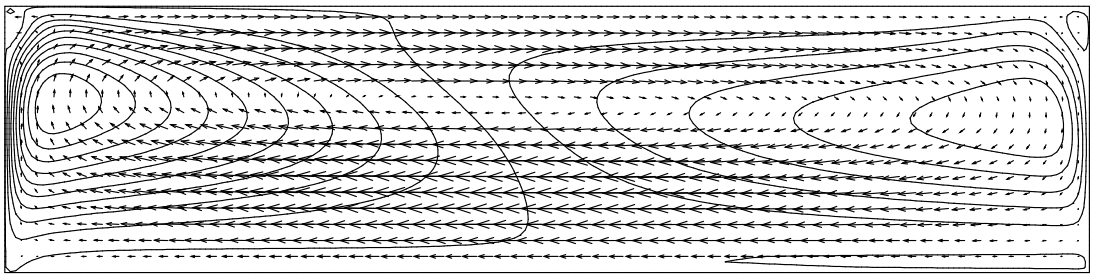

B

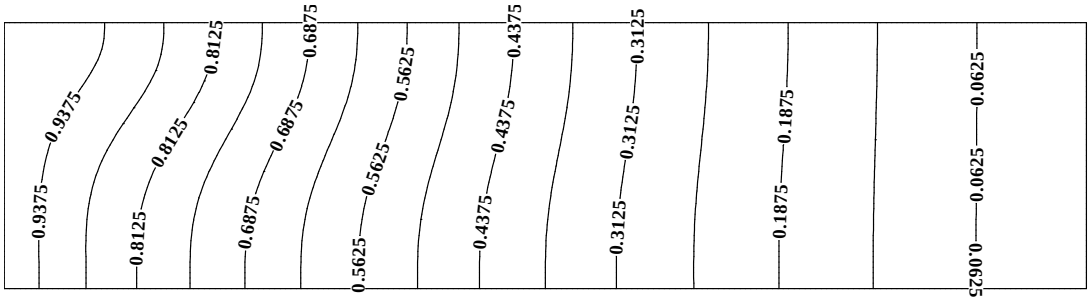
0.9375
0.8125
0.6875
0.5625
0.4375
0.3125
0.1875
0.0625

C

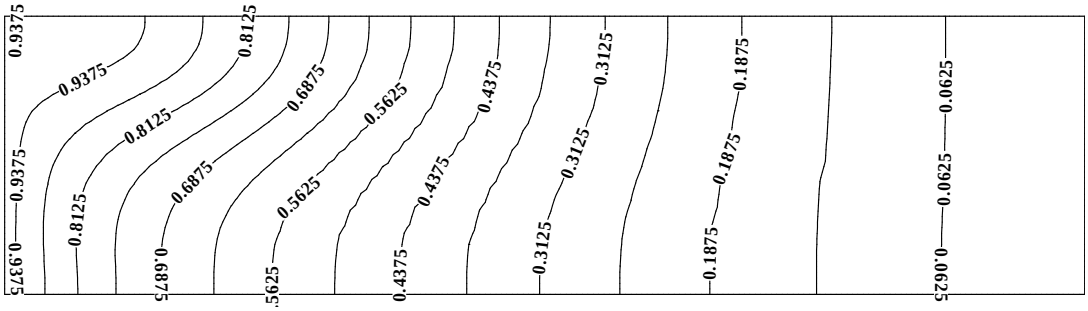
0.9375
0.8125
0.6875
0.5625
0.4375
0.3125
0.1875
0.0625

D

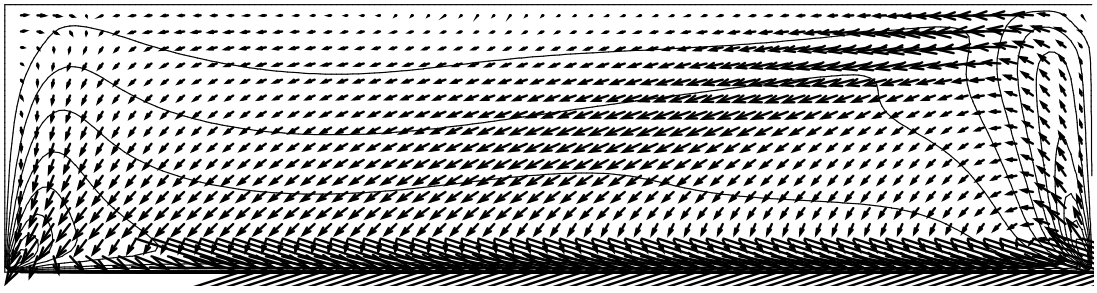

E

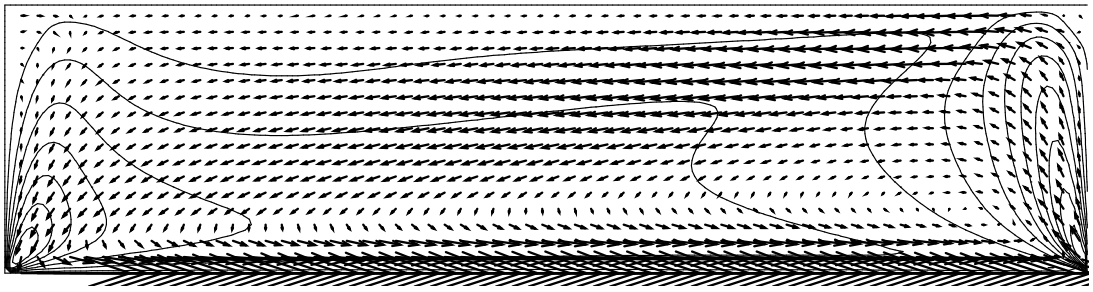

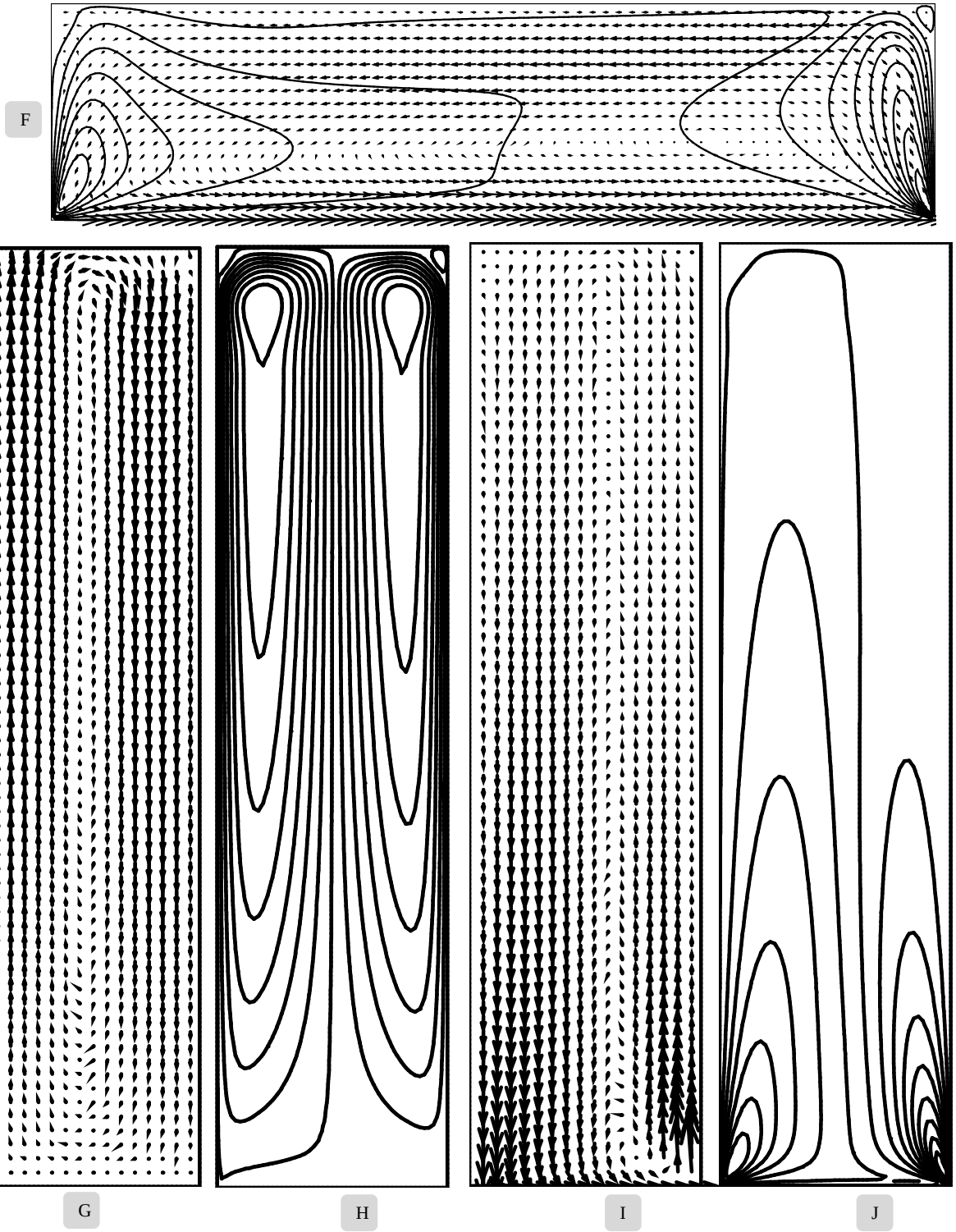

Fig. 6 Velocitiesdistributionsat different *Ra*and ε

Fig. 7 shows the velocities distributions (u) or x-component along the box *height*and (v) or y-component along the box *width*forAR = 0.25and 4.0 at Ra = 1000 and Da = 0.01 with and without lower wall-driven.Velocity components are plotted at mid width of the cavity and mid-height of the cavity respectively at different porosity.Fig. (7-A, B, C, and D) depicts x-components and y-components velocities forAR = 0.25and 4.0 respectively at ε = 0.4, 0.6, and 0.9 for the case of no movement.Fig. (7-E, F, G, and H) depicts x-components and y-components velocities forAR = 0.25and 4.0 respectively at ε = 0.4, 0.6, and 0.9 for the case of lower wall-driven. The effect of the moving wall is clear on the velocity distributions.The y-component velocity of flow is higher at the upper half of the cavity than that of bottom half. But for the x-component velocity is higher near the hot wall and it decreases continually with an increase in the horizontal distance.

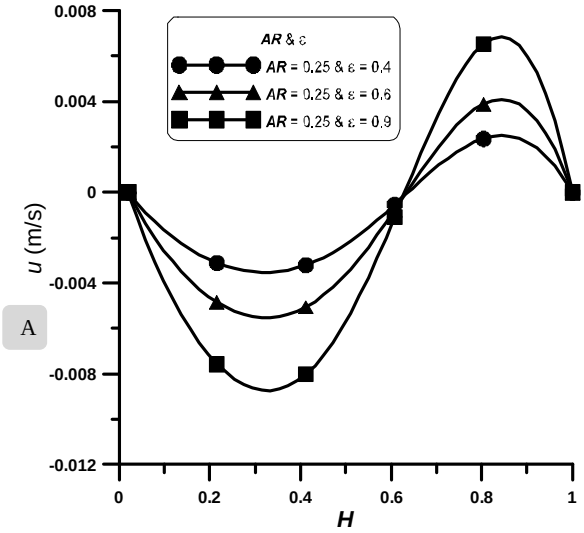

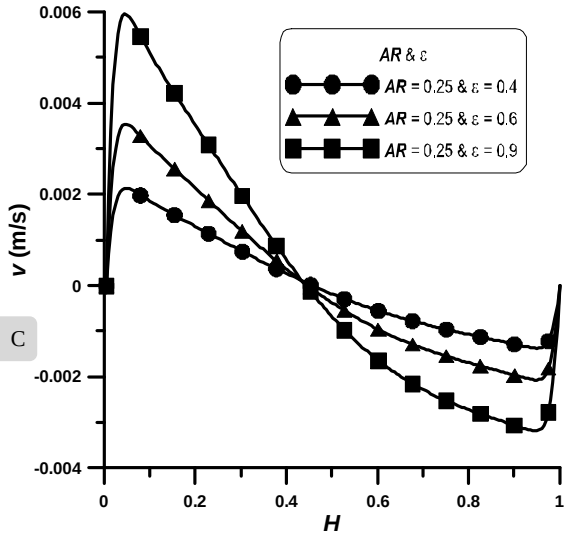

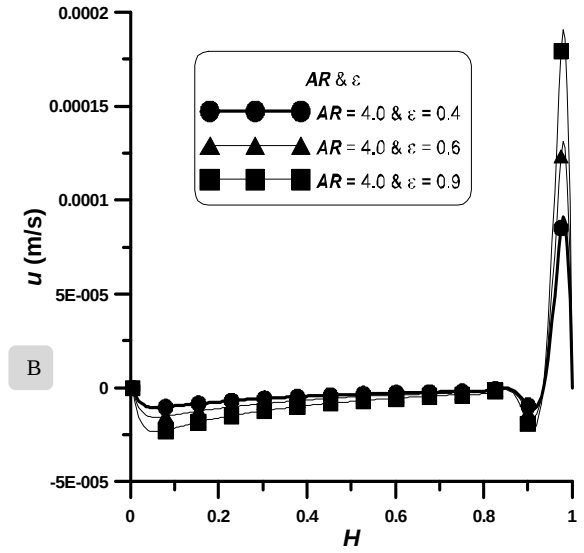

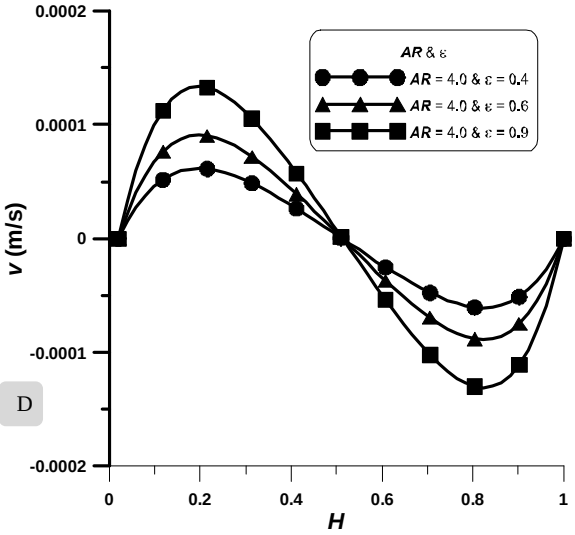

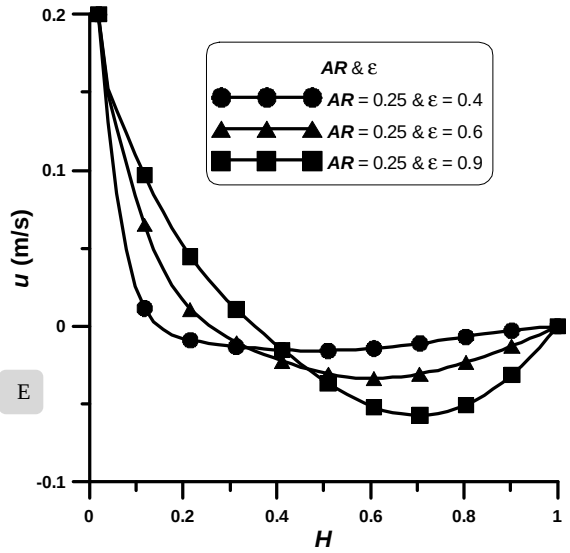

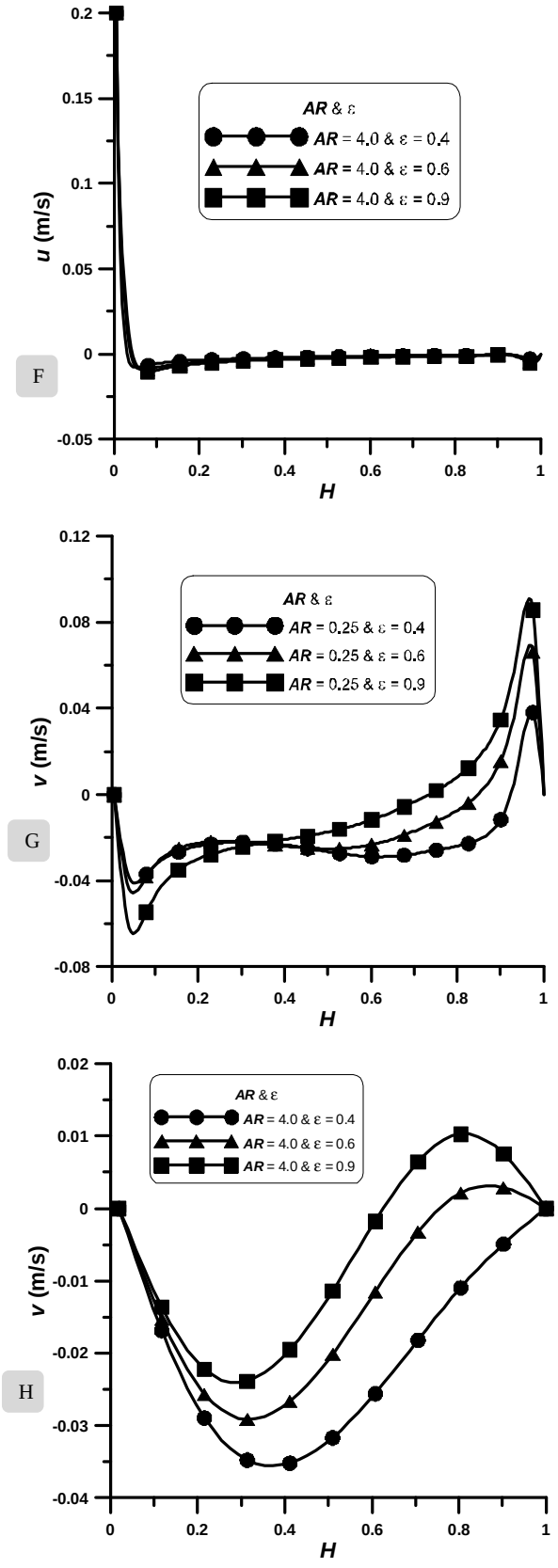

Fig. 7 Velocitiesdistributionsat different *Ra*and ε

Finally, table (1) tabulated theaverage Nusselt number $\overline{Nu}$ foraspect ratio and movement effects. The conclusions from this table are:

1- The highest average Nusselt number is in case (78) for*AR* = 0.25and ε = 0.9 with movement($\overline{Nu} \approx 3.2$) (i.e. moving the big horizontal wall).
2- Cases (73, 74, and 75) are refused because they reduce the average Nusselt number compared with *AR* = 1.0 (i.e. horizontal position without movement at *AR* = 0.25and ε = 0.4, 0.6, and 0.9).
3- The average Nusselt number increases as the porosity increases for the movement cases.
4- Atthe same porosity, as aspect ratio decreases the average Nusselt number decreases for no movement cases. And atthe same porosity, as aspect ratio decreases the average Nusselt number increases for movement cases.

TABLE I
AVERAGE NUSSELT NUMBER FOR ASPECT RATIO AND MOVEMENT EFFECTS

AR	ε	U_{lid} = 0.0 m/s	U_{lid} = 0.2 m/s
0.25	0.4	0.7884136	1.311706
	0.6	0.7170379	1.785798
	0.9	0.6652881	3.217035
1.0	0.4	0.9989753	1.222328
	0.6	0.9958305	1.591573
	0.9	0.9915955	2.031172
4.0	0.4	1.011749	1.051095
	0.6	1.011716	1.069172
	0.9	1.011661	1.088600

NOMENCLATURE

AR	Aspect ratio
c	Micro velocity vector
e	Discrete velocity
F	Total body force due to the presence of porous media
f_i	Discretized density distribution function
f_i^{eq}	Discretized equilibrium density distribution function
G	Boussinesq effect
g	Acceleration due to gravity
g_i	Discretized internal energy distribution function
g_i^{eq}	Discretized equilibrium internal energy distribution function
H	Characteristic length
j	Vertical direction opposite to that of gravity
K	Permeability
p	Pressure
T	Temperature
T_m	Average temperature

t	Time
U_{lid}	Moving lower wall velocity
u	Velocity vector
x	Position

Greek Symbols

β	Bulk coefficient
χ	Thermal diffusivity
Δt	Time step
ε	Porosity
ρ	Density
τ	Time relaxation
υ	Kinematic viscosity
υ_ε	Effective viscosity
ω	Weight coefficient

Non-dimensional Numbers

Nu	Nusselt number
Pr	Prandtl number
Ra	Rayleigh number
Da	Darcy number

REFERENCES

[1] Nithiarasu, P., Seetharamu, K. N. and Sundarajan, T., "Non-Darcy double-diffusive natural convectionin axisymmetric fluid saturated porous cavities," *Heat and Mass Transfer*,vol. 32, pp. 427-433, Springer-Verlag1997.

[2] Hakan F. Oztop, "Combined convection heat transfer in a porous lid-driven enclosure due to heater with finite length," *International Communications in Heat and Mass Transfer*, vol. *33*,pp.772 – 779,March 2006.

[3] Hakan F. Oztop, "Natural convection in partially cooled and inclined porous rectangular enclosures,"I*nternational Journal of Thermal Sciences*,vol.46, pp. 149–156, Elsevier 2007.

[4] Ayad F. Hameed, "Numerical Study of Free Convection Heat Transfer in a Cavity Filled With a Heat GeneratingSaturated Porous Medium," *Engineering and Technology Journal*, vol. 26,no. 4, pp.169–187, 2008.

[5] C.Y. Wang, "The recirculating flow due to a moving lid on a cavity containing a Darcy–Brinkman medium," *AApplied Mathematical Modelling*, vol.*33*,pp.2054–2061, 2009.

[6] M.A. MohdIrwan, A. M. Fudhail, C.S. Nor Azwadi and G. Masoud, "Numerical Investigation of Incompressible Fluid Flow through Porous Media in a Lid-Driven Square Cavity," *American Journal of Applied Sciences*, vol. *7*,no. *10*, pp. 1341-1344, 2010.

[7] Mohamed A. Teamahand Wael M. El-Maghlany, "Numerical simulation of double-diffusive mixed convective fl ow in rectangular enclosure with insulated moving lid," *International Journal of Thermal Sciences*, vol.*49*, pp.1625-1638, 2010.

[8] MohdIrwan Bin MohdAzmi, "Numerical Study of Convective Heat Transfer and Fluid Flow through Porous Media," *Masterthesis*, University Technology Malaysia, 2010.

[9] M. A. Waheed, G. A. Odewoleand S. O. Alagbe, "Mixed Convective Heat Transfer In Rectangular Enclosures Filled With Porous Media," *ARPN Journal of Engineering and Applied Sciences*, vol. 6, no. 8, pp.47-60, August 2011.

[10] Prakash Chandra and V. V. Satyamurty, "Non-Darcian and Anisotropic Effects on Free Convection in a Porous Enclosure," *Transp Porous Med*,vol. 90, pp. 301-320, May 2011.

[11] Antonio F. MIGUEL, "Non-Darcy Porous Media Flow in No-Slip and Slip Regimes," *THERMAL SCIENCE*,vol. 16, 6, no. 1,pp. 167-176, 2012.

[12] Wenchao Liu, Jun Yao and Yueying Wang, "Exact analytical solutions of moving boundary problems of one-dimensional flow in semi-infinite long porous media with threshold pressure gradient," *International Journal of Heat and Mass Transfer*,vol. 55, pp. 6017–6022, 2012.

[13] Laith J. Habeeb, "Numerical Simulation of Convective Heat Transfer and Fluid Flow through Porous Media with Different Moving and Heated Walls," *The XXXIII International Conference on Aerospace, Mechanical, Automotive and Materials Engineering*, Germany 2012, submitted for publication.